Korean J. Chem. Eng., **27**(6), 1700-1706 (2010)
DOI: 10.1007/s11814-010-0259-7

Reaction kinetics of phenol synthesis through one-step oxidation of benzene with N_2O over Fe-ZSM-5 zeolite

Guanjie Mi, Jianwei Li†, Jie Zhang, and Biaohua Chen

State Key Laboratory of Chemical Resource Engineering, Beijing University of Chemical Technology, Beijing 100029, China
(*Received 23 November 2009 • accepted 26 January 2010*)

Abstract–Based on the information from GC-MS on-line measurement and thermodynamic analysis, the reaction network of gas-phase hydroxylation of benzene with nitrous oxide over Fe-ZSM-5 zeolite was systematically investigated. The main reactions and side reactions were identified, and a kinetic reaction network was proposed as follows: benzene+N_2O→phenol→CO/CO_2. According to the mechanism, the experimental results were interpreted reasonably. The hydroxylation kinetic experiments were carried out in an isothermal integral microreactor under the conditions of n(benzene)/n(N_2O)=8-12, T=663-763 K and atmospheric pressure. Based on the reaction network proposed, the parameters in the rate model of power-law were estimated by means of Gauss-Newton optimal method with the Levenberg-Marquardt modifications, and the results were in good agreement with the experimental data.

Key words: Benzene, N_2O, Phenol, Oxidation, Reaction Kinetics, Reaction Network, Fe-ZSM-5 Zeolite

INTRODUCTION

Phenol is well known to be one of the most important chemicals among the fields of petrochemicals, agrochemicals, pharmaceuticals, and plastics. Examples of using phenol as an intermediate are in the production of bisphenol A, phenolic resins, caprolactam, alkylphenols, and aniline. More than 90% of the world production of phenol is obtained by the oxidation of cumene to form cumene peroxide, which is then cleaved into phenol and acetone in a three-step process involving oxidation of cumene. The first step is the alkylation of benzene with propylene to cumene in the presence of zeolite-based catalysts. The reaction can also be performed with Friedel-Crafts catalysts such as aluminium trichloride at 373-473 K. Then the cumene is converted to cumene peroxide in a non-catalytic auto-oxidation reaction. The last step is acidic cleavage of cumene hydroperoxide into phenol and acetone that is catalyzed by sulfuric acid at 333-373 K [1]. The advantage of the cumene process is that it takes two inexpensive starting materials, benzene and propylene, and converts them into two high value useful products, phenol and acetone, only using air. Despite its great success, the cumene process suffers from some drawbacks such as an explosive intermediate, i.e., cumene hydroperoxide, a high environmental impact, and a corrosive catalyst. It is a multi-step process, which makes it difficult to achieve high phenol yields in relation to the benzene used and which leads to a high capital investment. The most important problem is the co-production of acetone in 1 : 1 stoichiometry, i.e., 0.6 tons/ton of phenol produced. But the acetone market demand is much smaller than that of phenol. Therefore, the economic efficiency of the cumene process strongly depends on the demand for acetone in the chemical market. For this reason, new processes based on the direct oxidation of benzene are highly desirable. However, many attempts to accomplish one-step direct oxidation of benzene by various oxidants have not been successful. The interaction with O_2 in the presence of known catalysts leads mainly to the destruction of the aromatic ring and low phenol selectivity [2-7]. The most promising results seem to derive from the use of alternative oxidants as nitrous oxide, and the most active and selective catalyst for one-step direct oxidation of benzene by nitrous oxide is Fe-ZSM-5 zeolite, which provides nearly above 90% selectivity [8-16]. The first of such processes was realized by the cooperation of the Boreskov Institute of Catalysis (BIC) and Solutia Inc. (formerly a chemical business of Monsanto separated in 1997) in the late 1990s [17-20]. The process called AlphOx™ was originally developed to use the N_2O co-produced from the adipic acid plant to hydroxylate benzene to phenol, which is then hydrogenated to cyclohexanone and reintroduced into the adipic acid synthesis cycle. The AlphOx™ process shows several advantages when compared to the cumene process: one step only, low capital expenses, no acetone byproduct, avoiding N_2O emissions (a powerful greenhouse gas [16,21-23]), and no highly reactive intermediates. Nowadays, most of the studies reported in the literature focus on the development of catalyst, the modification of performance, and the optimization of reaction conditions in the case of one-step oxidation of benzene with N_2O. The kinetics for H-Ga-ZSM-5 catalyst has been studied more thoroughly [24,25]. However, the literature references regarding the kinetics of benzene to phenol oxidation with nitrous oxide over Fe-ZSM-5 zeolite are rather scarce. Although there is a general consensus concerning benzene oxidative hydroxylation, some controversies exist in the case of the reaction mechanism, the rate equations and kinetics parameters, which probably can be attributed to deviations in catalyst composition and structure. Kinetic study of the benzene oxidative hydroxylation can yield important information about the reaction mechanism. Even though the kinetics studies cannot determine the molecular mechanism, they allow the exclusion of possible reaction pathways and help obtain a quantitative analysis

†To whom correspondence should be addressed.
E-mail: lijw@mail.buct.edu.cn

for the participation of particular reaction routes and different catalytic sites in the proposed mechanism.

On the basis of our extensive experimental isothermal data on the oxidation of benzene gained in a laboratory fixed bed reactor with plug-flow behavior and without the influence of heat and mass transport limitations, the aim of this work was to find the rate equations that described the system behavior on Fe-ZSM-5 catalyst in the operating conditions for the design and/or simulation of an industrial reactor and obtain the elementary reaction pathways of the hydroxylation of benzene with N_2O over Fe-ZSM-5 zeolite.

EXPERIMENTAL

1. Catalyst

The catalysts were prepared by addition of Fe^{3+} ions to commercial zeolites. As starting material, zeolites of ZSM-5 type in the H-form with SiO_2/Al_2O_3 ratio of 25 were used, which were supplied by the Catalyst Plant of NanKai University. Iron was introduced by liquid ion-exchange method, which has already been described and has been used by other groups in a similar way [26-28]. The suspension (300 ml of a 1.448 g solution of $Fe(NO_3)_3$, 20 g H-ZSM-5 zeolite) was continuously stirred at 363 K for 3 h in a 500 ml flask and then the zeolite was recovered by filtration. The filtered solution was analyzed by atomic absorption spectroscopy to check whether the iron was completely ion-exchanged by the zeolite. The zeolite was washed with deionized water, as long as no more nitrate was detectable in the filtrate, dried at 373 K overnight, and the calcined at 913 K in air for 4 h with a heating rate of 10 K/min. Finally, steam treatment was performed with a water partial pressure of 300 mbar at 923 K for 4 h for all samples, again applying 10 K/min to heat the sample from room temperature to 923 K. Prior to the catalytic runs, the samples were pelletized without the binder and crushed to a size fraction of 0.18-0.30 mm.

The specific surface area and the specific pore volume of the samples, estimated by adsorption-desorption of N_2 at 77 K using the BET method with an ThermoFinnigan Sorptomatic 1990 device, were found to be 312.83 $m^2 \cdot g^{-1}$ and 0.1956 $cm^3 \cdot g^{-1}$, respectively.

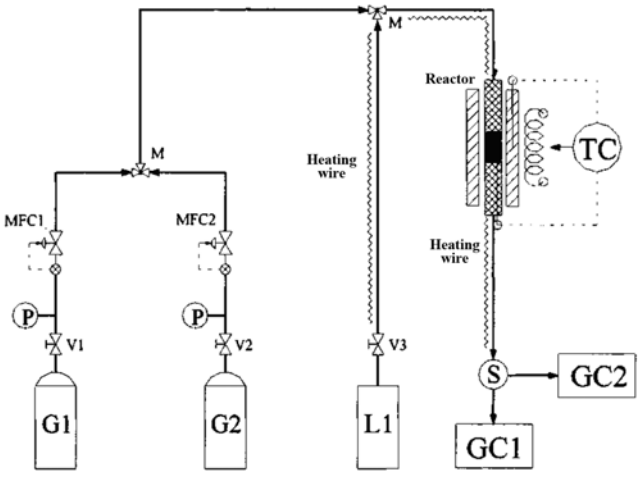

Fig. 1. Schematic diagram of the experimental setup. G1, He; G2, N_2O; L1, benzene; V1-V3, valves, MFC1-MFC2, mass flow controllers; M, mixer; S, separator.

Considering that an iron monolayer coverage corresponds to about 3.44×10^{17} molecules of iron per m^2 of specific surface area.

2. Experimental Setup

The experimental setup, shown in Fig. 1, consisted of three parts: feed mixing, reactor, and analysis zones. The kinetic studies were performed at atmospheric pressure using a continuous fixed-bed plug flow reactor equipped with chromatographic analysis of the feed and exit gas streams. For each experiment, 0.430 g catalyst particles were placed into a stainless steel reactor with the inner diameter of 6 mm. Before the measurements, the catalyst was activated in flowing helium for 5 h at 773 K. The kinetic experiments were conducted between 663 K and 763 K with varying inlet partial pressures of N_2O (5.38-7.11 kPa), benzene (55-64.62 kPa), and the balance helium. The choice of experimental conditions allowed the study of benzene/N_2O ratios ranging from 8/1 to 12/1. The reactor was equipped with a coaxial thermocouple in a thermowell located in the middle of the catalytic bed for temperature monitoring. Medical grade N_2O and high purity benzene were used as reagents. The feed gas component flow rate of each N_2O and He was controlled by mass flow controllers (Beijing Sevenstar Electronics Instruments). Benzene feed rate was controlled with an NP-KX-500 high-precision pump (Japanese Precision Scientific Instruments), which supplied liquid benzene to a feed vaporizer. The vaporized benzene was combined with N_2O and He feed streams upstream of the reactor inlet.

The exit gas mixture of the reactor was manually sampled and analyzed each 10 min. Samples were separated into the two phases by a condenser. The liquid fraction was analyzed by gas chromatography using a Varian GC3900 chromatograph, equipped with a OV-101 capillary column (50 m×0.25 mm, 0.5 μm) and a flame ionization detector. The gas fraction was analyzed with a stainless steel TDX-01 column (1.5 m×4 mm) and a thermal conductivity detector. The carbon mass balance was always less than 5%.

RESULTS AND DISCUSSION

1. Thermodynamics

Thermodynamics as intrinsic and fundamental characteristic of the reaction system is a crucial factor for the occurrence of chemical reaction and the formation of the target product with highest yield. In general, if a chemical reaction cannot occur spontaneously in view of thermodynamics, a discussion on the kinetics of the reaction system is ultimately insignificant. Therefore, probing into the thermodynamics of phenol formation procedure using benzene and nitrous oxide as feedstock over Fe-ZSM-5 zeolite has highly important significance for further academic investigation and practical applications. In a reaction system where there is more than one reaction pathway, there may be several possible routes to obtain the desired products and by-products. Based on the analysis of the by-products of the reaction system and the formation of carbonaceous deposits on the catalyst by GC-MS measurement, the catalytic oxidation of benzene to phenol with N_2O over Fe-ZSM-5 can be described by reactions (1)-(8) as follows:

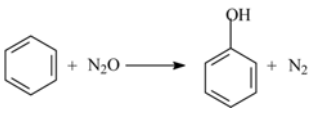

(1)

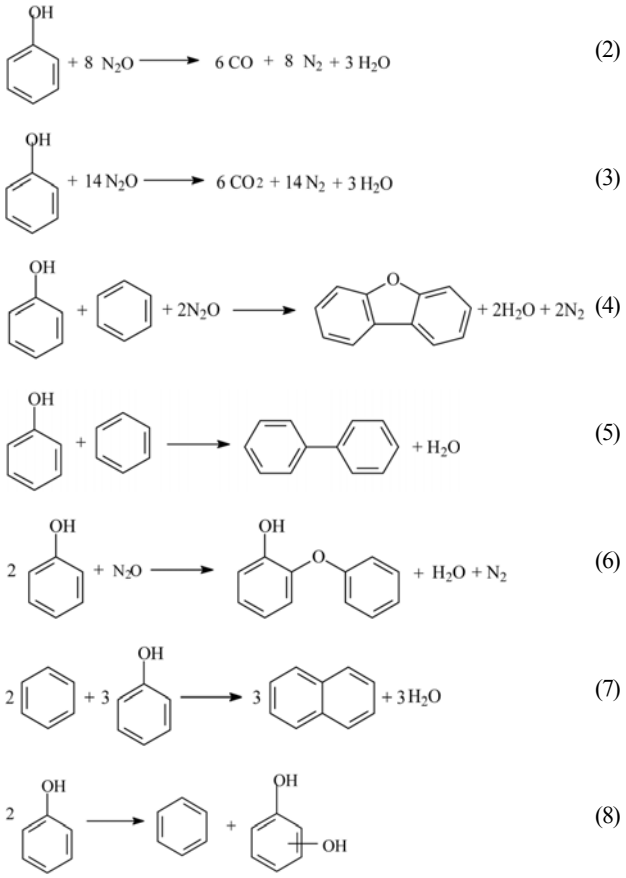

The thermodynamic data of various substances, such as the standard formation enthalpy ($\Delta_f H_m^{\Theta}$), the standard Gibbs free energy ($\Delta_f G_m^{\Theta}$) and the heat capacity $C_{p,m}^{\Theta}$, used in estimation of thermodynamic function changes of the reaction were found in the literature [29-31], or they were estimated using group additivity methods [32-34]. Hence, the heat and Gibbs function change of the reactions at different temperatures were estimated from their $\Delta_f H_m^{\Theta}$ and $\Delta_f G_m^{\Theta}$ values, as shown in Fig. 2 and Fig. 3, respectively.

Obviously, the reaction mechanism proposed except reaction (4) provided negative reaction enthalpy changes, suggesting that the reactions were exothermic. Moreover, the reaction enthalpy changes

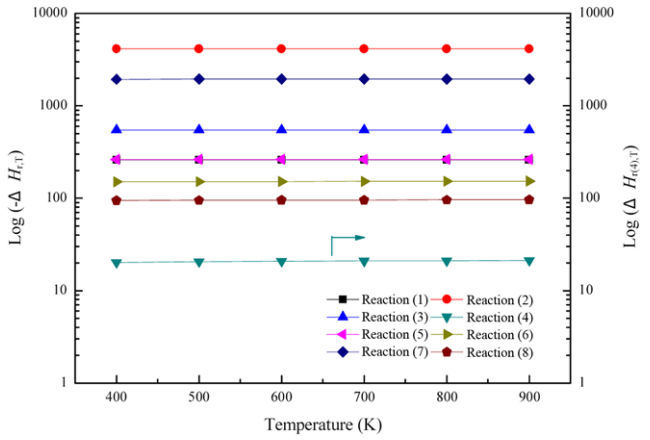

Fig. 2. The enthalpy changes in the conversion reactions of benzene to phenol by N_2O.

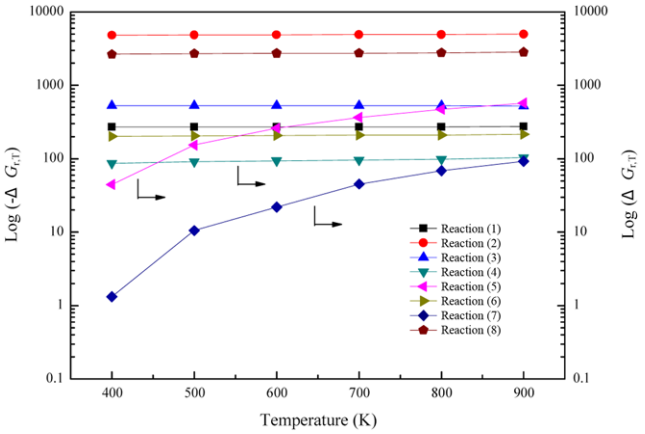

Fig. 3. The Gibbs free energy changes in the conversion reactions of benzene to phenol by N_2O.

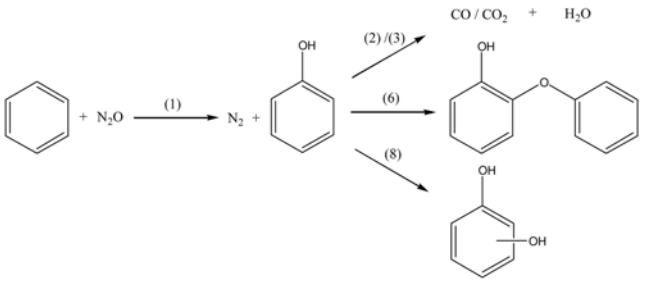

Fig. 4. Reaction network in the conversion of benzene with N_2O over Fe-ZSM-5 catalyst.

were not notably different at various temperatures. As it is reflected from the positive value of the Gibbs free energy changes of reactions (4), (5) and (7) in Fig. 3, the reaction processes were thermodynamically not feasible and non-spontaneous nature in a wide temperature range. On the contrary, the rest of the reactions provided the negative Gibbs free energy changes, indicating that the reactions were thermodynamically feasible and spontaneous. Besides, the Gibbs free energy changes of the reactions, namely reaction (1), (2), (3), (6) and (8), were far less than zero, so the reactions can all be considered as the irreversible reactions. Thus, on the basis of the above thermodynamic calculations a complex reaction network can be concluded and shown in Fig. 4:

First, benzene and N_2O were adsorbed in the Fe-ZSM-5 zeolite, then N_2O was activated upon the formation of an active oxygen species at an active site under the release of nitrogen. Apart from the hydroxylation of adsorbed benzene to phenol by the chemisorbed oxygen species as the main reaction, the consecutive reaction of phenol may be either the non-selective oxygenation adsorbed phenol by chemisorbed oxygen and the transformed to CO/CO_2 or may react with N_2O or another phenol molecule to give the products of coupling. The by-products were detected by GC-MS in the adsorbing organic solution collecting the gas stream out of the reactor. It should be noted that the by-products, such as phenyl-2-phenoxy and dihydroxybenzene, can be detected only after long reaction time and present in a very small amount. So in principle, it was reasonable to rule out the reactions of the by-products, i.e., reactions (6) and (8), in the next kinetic study. Therefore, it was believed that

reactions (1), (2) and (3) constituted the determinative simple kinetic equations.

2. Kinetics for Phenol Synthesis from Benzene Hydroxylation

2-1. Reactor Model

For the utilization of an ideal, isothermal, pseudo homogeneous fixed bed reactor with plug flow behavior model, it was necessary to verify the criteria for the plug flow and also to examine whether the effect of the external and internal diffusion on the kinetics of reaction could be neglected.

Conventional criteria for ideal plug flow were

$d_r/d_p>10$, $L/d_p>50$ and $Re=(\rho u d_p)/\mu>10$

For the kinetic experimental conditions employed in the present work, it followed that $d_r/d_p=25$ and $L/d_p=125$. Also, typical Reynolds numbers in the present study were all more than 10. Hence, the plug flow can be assumed.

Preliminary experiments performed at the higher reaction temperature studied (673 K) with varying total space velocity ensured the absence of external mass transfer limitations for space velocity ≥8,000 ml(gas)·(ml(cat)·h)$^{-1}$, as shown in Fig. 5. Since the Fe-ZSM-5 catalyst used in this study has a very small particle size (<0.375 mm), the internal transfer limitations were assumed to be negligible, as shown in Fig. 6. The absence of heat transfer limitation on the kinetics was also confirmed theoretically, based on the criteria given by Dekker et al. [35]. The resulting mass balance of the ideal plug-flow tubular reactor for each gas phase component was expressed by the following Eq. (9):

$$-\frac{d(c_i u)}{dz}+\sum_j^k \nu_{i,j} r_j = 0 \tag{9}$$

where r_j was the reaction rate of the j reaction, $\upsilon_{i,j}$ was the stoichiometric coefficient of the component i in reaction j, z was the axial reactor coordinate, c_i was the concentration of the component i, and u was the gas linear velocity, resulting in a first-order differential equation system.

The initial condition for Eq. (9) was given as

at $z=0$, $c_i=c_{i0}$.

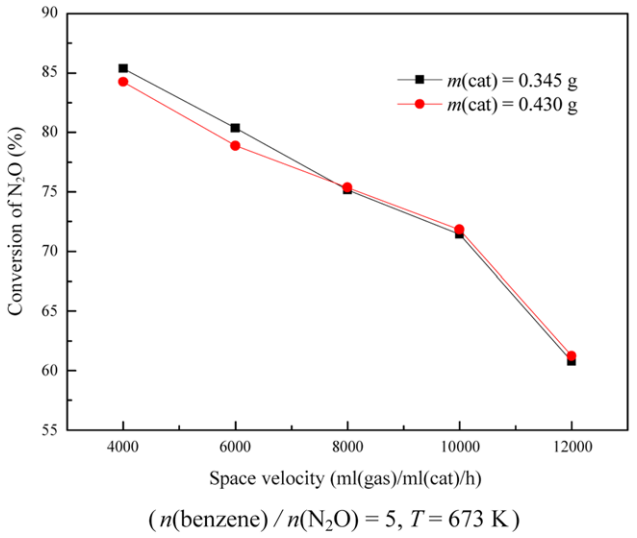

(n(benzene) / n(N_2O) = 5, T = 673 K)

Fig. 5. External diffusion test of Fe-ZSM-5 zeolite catalyst particles.

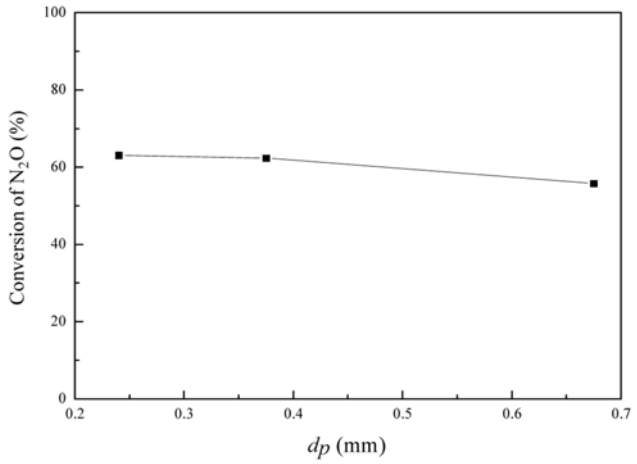

(n(benzene) / n(N_2O) = 5, T = 673 K)

Fig. 6. Internal diffusion test of Fe-ZSM-5 zeolite catalyst particles.

2-2. Kinetic Model

As discussed in Section 3.1, the reaction network consisted of three reactions: (1) the selective oxidative hydroxylation of benzene to phenol, (2) the consecutive oxidation of phenol to carbon monoxide, and (3) the total consecutive oxidation of phenol to carbon dioxide. The rate of each of these reactions can be expressed in the power-law models as follows:

$$r_1 = k_{01}\exp\left(-\frac{E_1}{R_g T}\right) y_B^{a_1} y_{N_2O}^{b_1} \tag{10}$$

$$r_2 = k_{02}\exp\left(-\frac{E_2}{R_g T}\right) y_{Ph}^{a_2} y_{N_2O}^{b_2} \tag{11}$$

$$r_3 = k_{03}\exp\left(-\frac{E_3}{R_g T}\right) y_{Ph}^{a_3} y_{N_2O}^{b_3} \tag{12}$$

The mole fractions of benzene (y_B), nitrous oxide (y_{N_2O}) and phenol (y_{Ph}) were used to calculate the reaction rate.

Although the power-law model did not provide any fundamental information on the reaction mechanism, it adequately predicted the main trends of the reaction and provided a good fitting of the experimental results. Moreover, it was often very useful from an engineering standpoint for directly evaluating the effect of the operation variables on reactor performance.

2-3. Parameter Estimation

On the basis of 40 kinetic experimental data in the plug flow reactor, a portion of which are listed in Table 1, the kinetic parameters were fitted to the experimental values. The postulated rate expressions led to mathematical models that were highly nonlinear with respect to their parameter. Therefore, parameter estimation was performed using the nonlinear least-squares regression routine nlinfit.m, which is available in the optimization toolbox of MATLAB, version R2008a. This routine uses the Gauss-Newton algorithm with the Levenberg-Marquardt modifications for global convergence. The objective function based on the squares sum of relative difference between experimental and calculated mole fraction of components was defined as follows:

Table 1. Experimental kinetic data for gas-phase hydroxylation of benzene with N_2O over Fe-ZSM-5 zeolite

T (K)	n_i (mol/h)	y_i (B) (%)	y_i (N_2O) (%)	y_o (N_2) (%)	y_o (CO) (%)	y_o (CO_2) (%)	y_o (N_2O) (%)	y_o (B) (%)	y_o (Ph) (%)	y_o (H_2O) (%)
690.2	0.675	57.60	6.40	2.55	0.01	0.05	2.71	61.56	3.32	0.03
688.8	0.671	58.18	5.82	2.31	0.01	0.06	2.55	62.84	2.60	0.04
690.9	0.690	58.67	5.33	2.36	0.03	0.05	1.78	64.34	2.58	0.04
667.1	0.548	55.00	5.00	1.86	0.01	0.04	2.48	58.09	2.01	0.02
692.1	0.555	55.00	5.00	2.86	0.05	0.06	1.47	56.76	2.54	0.05
716.2	0.573	55.00	5.00	3.62	0.08	0.09	0.55	57.82	3.37	0.09
738.0	0.561	55.00	5.00	4.04	0.17	0.13	0.09	56.26	3.75	0.15
710.7	0.567	56.00	7.00	3.65	0.11	0.10	2.13	58.09	3.68	0.11
737.8	0.565	56.00	7.00	5.00	0.07	0.13	0.47	56.38	4.66	0.10
763.5	0.585	56.00	7.00	5.44	0.11	0.21	0.12	57.41	4.64	0.16

Subscript: i-reactor inlet, o-reactor outlet

$$F_{obj}=\sum_{i=1}^{n}\sum_{j=1}^{m}\left(\frac{y_{i,j}^{e}-y_{i,j}^{c}}{y_{i,j}^{e}}\right)^2 \quad (13)$$

In the equation, superscripts e and c indicate experimental and calculated values, respectively. Subscripts i and j stand for the key components and the ordinal number of kinetic experiments, respectively.

The system of differential equations was numerically integrated over the catalyst mass for each set of initial experimental conditions, using the 4^{th} order Runge-Kutta method by the function ode45. In the parameter search procedure, the objective function was to minimize the sum of the squared differences between the experimental molar fractions for each key species and their fitted values. The minimization was performed by first obtaining an initial estimate of the kinetic parameters using a genetic algorithm [36,37]. The big advantage of genetic algorithms is that they are able to depart from local minima, thus obtaining with high probability a global solution. Moreover, nlparci was used to produce the 95% confidence interval for each estimated parameter. The kinetic parameters, with the 95% confidence intervals, obtained for the power-law model are tabulated in Table 2. Now a model for phenol synthesis from benzene on Fe-ZSM-5 catalyst was obtained and it can be used to predict the distribution of the components.

The nonselective oxidation reactions of phenol to CO/CO_2 had a much higher reaction power than the selective oxidation reaction, conforming to the consecutive reaction mechanism of phenol to CO/CO_2. Concerning the effect of N_2O concentration in the feed, we can see that in the nonselective oxidation of produced CO/CO_2, N_2O had a higher effect on the reaction rates. Thus, decreasing the N_2O concentration in the feed stream proved beneficial for increasing the selectivity and the yield of phenol. Furthermore, the activation energy for the benzene oxidation to phenol was lower than the activation energies of the two other reactions; therefore, the selectivity to phenol was expected to decrease with increasing temperature.

Table 2. Regression parameters and F-test of the kinetic model

Equation	k_0 (mol/(gcat)/h)	E (kJ/mol)	a	b	F	$10F_{0.05}$
(10)	3.91×10^4	14.07	0.85	0.24	163.2	
(11)	3.12×10^4	92.51	0.91	0.49	141.6	17.2
(12)	2.03×10^4	83.38	1.04	1.62	147.7	

2-4. Kinetic Model Verification

Statistical measures for the model have been done and its relevant parameters were computed to identify their significance. The square of the correlation between the response values and the predicted response values (R^2) measurements for Eqs. (10) to (12) were 0.9541, 0.9301 and 0.9381, respectively, and were all greater than 0.9, indicating statistically significant. Besides, F measurements, which are based on the comparison of the sum of squares of the calculated response values and the residual sum of squares, were all greater than $10F_{\alpha}(\alpha=0.05)$ for every rate model, as shown in Table 1. The comparisons between the model predictions to the mole fraction of components and the experimental data were also investigated, as shown in Figs. 7 to 9. It was seen that the concentrations predicted by the model were all in good agreement with the data obtained in a wide range of experimental conditions. The parity plots did not show any systematic deviations, with all points equally spread around the diagonal line, indicating that the deviations were attributed to the experimental, not the model-based, error. With the exception of a few points, the deviations were within 10%, and for most

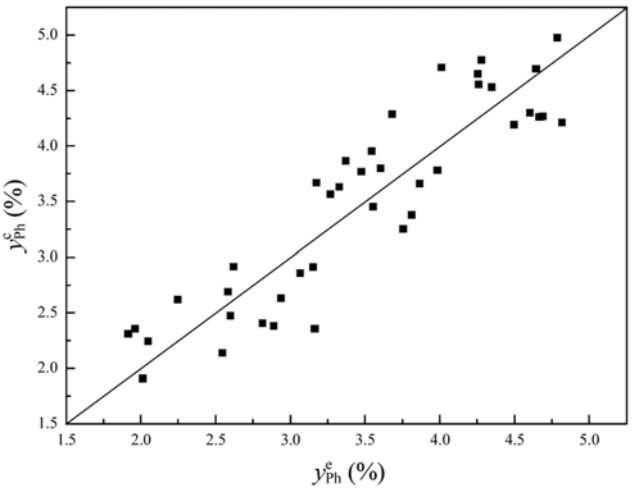

Fig. 7. Comparison between experimental phenol molar percentage and the calculated from Eq. (10) at the reactor output.

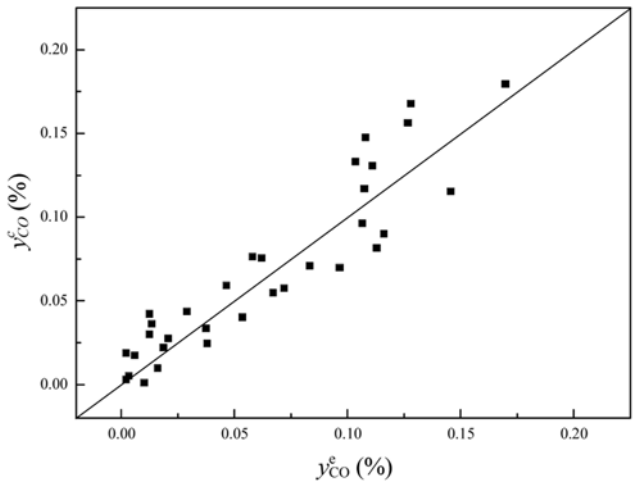

Fig. 8. Comparison between experimental CO molar percentage and the calculated from Eq. (11) at the reactor output.

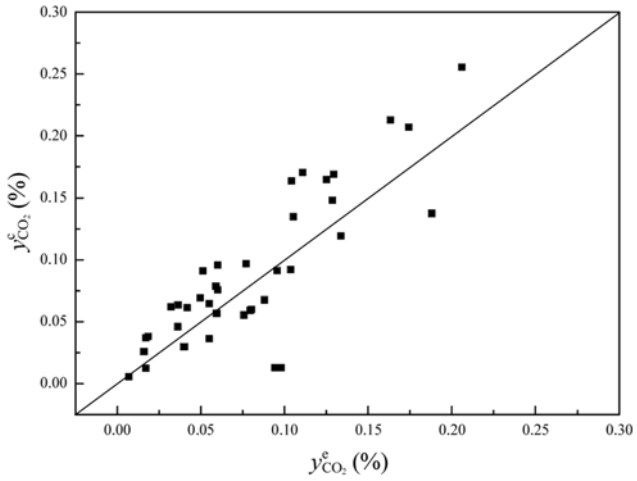

Fig. 9. Comparison between experimental CO_2 molar percentage and the calculated from Eq. (12) at the reactor output.

data, they were significantly smaller. All statistical measures revealed that the model proposed was acceptable from the viewpoint of application.

CONCLUSION

Fe-modified ZSM zeolite, which has been shown to have high activity and selectivity in a previous study of the authors, offered a viable heterogeneous solid base catalyst for the hydroxylation of benzene with N_2O to phenol. Intrinsic kinetic experiments were performed between 663 and 763 K at atmospheric pressure and different space time with pure component feeds and different feed compositions. The proposed reaction rate expressions were based on the GC-MS on-line measurement and thermodynamic analysis of the reaction system. The kinetic model based on a power-law type of mechanism consisting of three reaction steps was found to give a satisfactory description of the experimental data over the investigated range of experimental conditions. The estimation of the kinetic parameters was performed by minimization of the squares sum of relative difference of the response variables with the Gauss-Newton algorithm with the Levenberg-Marquardt modifications. The obtained parameters were statistically significant and a good agreement between simulated and experimental values was observed. The data of reaction orders and activation energies suggested that lower N_2O concentration in the feed stream and reaction temperatures would be beneficial for increasing the selectivity of the reaction to form phenol.

ACKNOWLEDGEMENT

We gratefully acknowledge the financial support of the National Natural Science Funds for Distinguished Young Scholar (20625621).

NOMENCLATURE

a, b : reaction order
c : gas-phase concentration of a component [$mol \cdot m^{-3}$]
$C^{\Theta}_{p,m}$: standard heat capacity [$J \cdot mol^{-1} \cdot K^{-1}$]
d_p : particle diameter [m]
d_r : reactor diameter [m]
E : activation energy of reaction [$kJ \cdot mol^{-1}$]
F : Fisher's value
F_{obj} : objective function
$\Delta_f G^{\Theta}_m$: standard Gibbs free energy [$kJ \cdot mol^{-1}$]
$\Delta_f H^{\Theta}_m$: standard formation enthalpy [$kJ \cdot mol^{-1}$]
k_0 : reaction rate constant [$mol \cdot gcat^{-1} \cdot h^{-1}$]
L : catalyst bed length [m]
n : number of moles of a component [mol]
nlparci : stands for the function of producing the 95% confidence interval for each estimated parameter in Matlab software
ode45 : stands for the function of the 4th order Runge-Kutta method in Matlab software
r : reaction rate [$mol \cdot gcat^{-1} \cdot h^{-1}$]
Re : Reynolds number
R_g : universal gas constant [8.314 $kJ \cdot mol^{-1} \cdot K^{-1}$]
R^2 : complex correlative index
T : temperature [K]
u : gas linear velocity [$m \cdot s^{-1}$]
y : molar fraction
z : axial reactor coordinate [m]

Greek Symbols

α : confidence level
ν : stoichiometric coefficient
μ : gas viscosity [$kg \cdot m^{-1} \cdot s^{-1}$]
ρ : density [$kg \cdot m^{-3}$]

Superscripts and Subscripts

c : calculated value
e : experimental value
i : component i
j : jth experimental point

REFERENCES

1. R. J. Schmidt, *Appl. Catal. A: Gen.*, **280**, 89 (2005).
2. I. Yamanaka, M. Katagiri, S. Takenaka and K. Otsuka, *Stud. Surf.*

Sci. Catal., **130**, 809 (2000).
3. E. Battistel, R. Tassinari, M. Fornaroli and L. Bonoldi, *J. Mol. Catal. A: Chem.*, **202**, 107 (2003).
4. R. Hamada, Y. Shibata, S. Nishiyama and S. Tsuruya, *Chem. Phys.*, **5**, 956 (2003).
5. N. I. Kuznetsova, L. I. Kuznetsova, V. A. Likholobov and G. P. Pez, *Catal. Today*, **99**, 193 (2005).
6. Y. Y. Liu, K. Murata and M. Inaba, *J. Mol. Catal. A: Chem.*, **256**, 247 (2006).
7. L. C. Passoni, A. T. Cruz, R. Buffon and U. Schuchardt, *J. Mol. Catal. A: Chem.*, **120**, 117 (1997).
8. L. V. Pirutko, A. K. Uriarte, V. S. Chernyavsky, A. S. Kharitonov and G. I. Panov, *Micropor. Mesopor. Mater.*, **48**, 345 (2001).
9. G. I. Panov, *CATTECH*, **4**, 18 (2000).
10. S. N. Vereschagin, N. P. Kirik, N. N. Shishkina, S. V. Moroz, A. I. Vyalkov and A. G. Anshits, *Catal. Today*, **61**, 129 (2000).
11. E. J. M. Hensen, Q. Zhu, M. M. R. M. Hendrix, A. R. Overweg, P. J. Kooyman, M. V. Sychev and R. A. van Santen, *J. Catal.*, **221**, 560 (2004).
12. Q. Zhu, R. M. van Teeffelen, R. A. van Santen and E. J. M. Hensen, *J. Catal.*, **221**, 575 (2004).
13. A. Waclaw, K. Nowinska and W. Schwieger, *Appl. Catal. A: Gen.*, **270**, 151 (2004).
14. J. Jia, K. S. Pillai and W. M. H. Sachtler, *J. Catal.*, **221**, 119 (2004).
15. K. S. Pillai, J. Jia and W. M. H. Sachtler, *Appl. Catal. A: Gen.*, **264**, 133 (2004).
16. V. N. Parmon, G. I. Panov, A. Uriarte and A. S. Noskov, *Catal. Today*, **100**, 115 (2005).
17. A. S. Kharitonov, G. I. Panov, K. G. Ione, V. N. Romannikov, G. A. Sheveleva, L. A. Vostrikova and V. I. Sobolev, US Patent, 5,110,995 (1992).
18. A. K. Uriarte, M. A. Rodkin, M. J. Gross, A. S. Kharitonov and G. I. Panov, *Stud. Surf. Sci. Catal.*, **110**, 857 (1997).
19. A. K. Uriarte, *Stud. Surf. Sci. Catal.*, **130**, 743 (2000).
20. P. P. Notté, *Top. Catal.*, **13**, 387 (2000).
21. J. Pérez-Ramírez, F. Kapteijn, K. Schöffel and J. A. Moulijn, *Appl. Catal. B: Environ.*, **44**, 117 (2003).
22. J. C. Groen, J. Pérez-Ramírez and W. Zhu, *J. Chem. Eng. Data*, **47**, 587 (2002).
23. M. Y. Kim, K. W. Lee, J. H. Park, C.-H. Shin, J. Lee and G. Seo, *Korean J. Chem. Eng.*, **27**, 76 (2010).
24. M. Häfele, A. Reitzmann, D. Roppelt and G. Emig, *Appl. Catal. A: Gen.*, **150**, 153 (1997).
25. M. Häfele, A. Reitzmann, E. Klemm and G. Emig, *Stud. Surf. Sci. Catal.*, **110**, 847 (1997).
26. G. Centi and F. Vazzana, *Catal. Today*, **53**, 683 (1999).
27. J. Cejka, B. Wichterlova, J. Krtil, M. Krivanek and R. Fricke, *Stud. Surf. Sci. Catal.*, **69**, 347 (1991).
28. R. Joyner and M. Stockenhuber, *J. Phys. Chem. B.*, **103**, 5963 (1999).
29. R. C. Reid, J. M. Prausnitz and B. E. Poling, *The properties of gases and liquids*, McGraw-Hill, New York (1987).
30. J. B. Pedley, R. D. Naylor and S. P. Kirby, *Thermochemical data of organic compounds*, Chapman and Hill, London (1986).
31. R. C. Weast, M. J. Astle and W. H. Beyer, *CRC handbook of chemistry and physics*, CRC Press, Florida (1988).
32. S. W. Benson, *Thermochemical kinetics: Methods for the estimation of thermochemical data and rate parameters*, John Wiley & Sons, New York (1976).
33. S. W. Benson, F. R. Crickshank, D. M. Golden, G. R. Haugen, H. E. O'Neal, A. S. Rodgers, R. Shaw and R. Walsh, *Chem. Rev.*, **69**, 279 (1969).
34. S. W. Benson, *J. Phys. Chem.*, **103**, 11481 (1999).
35. F. H. M. Dekker, A. Bliek, F. Kapteijn and J. A. Moulijn, *Chem. Eng. Sci.*, **50**, 3573 (1995).
36. Y. H. Kim, D.-Y. Hwang, S. H. Song, S. B. Lee, E. D. Park and M.-J. Park, *Korean J. Chem. Eng.*, **26**, 1 (2009).
37. A. de Luis, J. I. Lombraña, F. Varona and A. Menéndez, *Korean J. Chem. Eng.*, **26**, 48 (2009).